Sādhanā (2022)47:153
https://doi.org/10.1007/s12046-022-01929-9

An improved similarity-based residual life prediction method based on the dynamic variable combination

M Y GU* and J Q GE

College of Quality and Safety Engineering, China Jiliang University, Hangzhou, China
e-mail: gmycjlu@cjlu.edu.cn; 871756973@qq.com

MS received 5 December 2021; revised 2 May 2022; accepted 31 May 2022

Abstract. Remaining useful life (RUL) prediction is essential for preventive maintenance and industrial safety operation. As an emerging data-driven method, the similarity-based residual life prediction (SbRLP) method plays a vital role in the RUL prediction. However, its existing research usually adopts fixed variables without considering the sensitivity difference of the same variable in different degradation states, thus making locally insensitive variables unusable and resulting in a waste of valuable monitoring information. Therefore, to fully mine useful monitoring information to improve the RUL prediction accuracy, this paper proposed an improved SbRLP method based on the dynamic variable combination. Firstly, the K-means algorithm was employed to divide state intervals, and combined with state intervals, the dynamic variable combination was determined through the local sensitivity analysis. Then, the state interval was recognized by the multi-SVDD algorithm with a novel discrimination criterion, and united with the dynamic variable combination, the RUL was predicted through the SbRLP method. Eventually, a case study is provided to demonstrate the effectiveness and superiority of the proposed SbRLP method. The results show that the proposed SbRLP method has better prediction performance, especially during the equipment's early and mid-term performance degradation. Moreover, implementing the new discriminate criterion can help improve its prediction accuracy.

Keywords. Similarity-based; RUL prediction; dynamic variable combination; local sensitivity; state interval.

1. Introduction

With the operation of equipment, degradation-induced failure is inevitable [1]. If no actions can be taken timely, the equipment failure may result in severe economic loss and safety problems. For example, rolling bearing is an important part of modern industrial equipment, and its failures may cause the breakdown of the equipment. Obviously, unexpected failures should be avoided [2]. One helpful approach is conducting RUL prediction, which can aid operators in the maintenance decision-making process to take timely maintenance before irreversible damage. Therefore, RUL prediction has gained significant attention recently.

Current RUL prediction includes model-based and data-driven methods. The former predicts the RUL of the equipment by the mathematical model established with its physical failure mechanism, such as fatigue [3] and cracking [4]. This method has high prediction accuracy, but its failure mechanism modeling is difficult for complex equipment. Therefore, the model-based approach is more suitable for equipment with simple structures or known failure mechanisms. The latter establishes the RUL prediction model based on the equipment's monitoring data, and it is suitable for equipment with easily obtained full-life-cycle monitoring data [5]. Depending on the relationship between monitoring data and RULs, data-driven methods can be divided into state extrapolation, statistical regression, and SbRLP methods. State extrapolation methods extrapolate the development trends of monitoring variables through methods such as Kalman filters [6] and particle filtering method [7] and then predict the equipment RUL by comparison with their failure thresholds. Statistical regression methods utilize algorithms such as GKPCA [8], neural network [9], and SVM [10] to establish the mapping model between monitoring variables and RULs based on historical degradation data of similar equipment. The above two methods require much time and effort to select an appropriate prediction model because an inappropriate model will severely affect prediction accuracy. Moreover, the participation of new samples leads to the retraining of their prediction models. As an emerging data-driven technique, the SbRLP method predicts the RUL of the operating sample as a weighted aggregation of several reference samples' actual RULs. It can effectively avoid the burden of degradation modeling and has an excellent long-term prediction capability. Furthermore, Liu *et al* [11], Yu *et al* [12], and Wang *et al* [2] have demonstrated that it has

*For correspondence
Published online: 05 August 2022

better prediction accuracy and generalization than many algorithms. For example, Elman recurrent neural network (ERNN), auto-regressive moving average (ARMA), deep convolutional neural network (DCNN), multi-objective deep belief networks ensemble, hidden Markov model (HMM), and grey model (GM). You and Meng [13] have illustrated that it is more robust against noise than the sensory-updated degradation modeling method. These make the SbRLP method much more appealing in academics and industry.

Reliable health indicators (HIs) are the cornerstone for accurate similarity-based RUL prediction. According to the number of HIs, HI construction in similarity-based RUL prediction consists of one-dimensional and multi-dimensional HI construction. The former aims at extracting one-dimensional HI from high-dimensional monitoring data to reflect the equipment state. For example, Yu *et al* [12] proposed a recurrent neural network (RNN) auto-encoder to construct the HI curve. Malinowski *et al* [14] built the HI by multiple linear regression. Liu *et al* [15] employed principal component analysis (PCA) to process monitoring data and selected the first principal component as the HI. Hou *et al* [16] put forward an unsupervised machine learning algorithm—the restrained Boltzmann machine to construct the HI. Zhao and Chen [17] constructed the HI based on sensor parameters obtained by three criteria: the data variation range, the value difference at engine leaving the factory, and the value difference at engine removal. Liang *et al* [18] synthesized the HI based on the offset distance and angle between normal and operational states of the equipment. The latter refers to portraying the equipment state with two or more HIs. Compared with one-dimensional HI construction, there is less research on multi-dimensional HI construction because the number of HIs is closely related to the computational effort of subsequent similarity-based RUL prediction. For example, Wang *et al* [19] optimized candidate parameters through the genetic algorithm (GA) and fused optimal parameters into comprehensive indicators through the stacked sparse auto-encoder. Yu *et al* [20] obtained optimal sensor variables based on Lasso. Zhang *et al* [21] came up with four evaluation indexes to screen degradation variables: monotonicity, correlation, predictability, and robustness. Gu *et al* [22] balanced the degradation reflection effect and monitoring costs to develop the variable combination.

The abovementioned literature screened monitoring variables based on the differences in their sensitivity to the equipment degradation performance and therefore adopted constant variable combinations. However, the same monitoring variable has different sensitivities in different degradation states. For example, Zhang *et al* [23] hold that some variables are not sensitive to the initial equipment degradation, which means that some variables are global-sensitive and some are local-sensitive. Under this circumstance, local-insensitive variables may be unavailable if monitoring variables are screened based on their global sensitivities, resulting in a waste of valuable monitoring information. In summary, to fully mine usable monitoring information and improve the prediction accuracy of the SbRLP method, this paper proposes the concept of the dynamic variable combination, in which the number and type of available variables vary with the equipment state. Moreover, combined with the sensitivity difference of one monitoring variable in different state intervals, the dynamic variable combination is determined based on the local sensitivities of monitoring variables in different state intervals.

Effective state interval recognition is an important link in realizing the above idea. According to the recognition principles, existing state interval recognition methods contain knowledge-based, model-based, and data-driven methods. Knowledge-based and model-based methods require extensive mechanistic knowledge, making them difficult to achieve good results on complex equipment. With advances in information technology, data-driven methods have become the most popular because they can mine valuable information from monitoring data without demanding mechanistic knowledge. Commonly-used data-driven methods include neural networks [24], support vector machine (SVM) [25], self-organizing map model (SOMM) [26], continuous hidden semi-Markov model (CHSMM) [27], support vector data description (SVDD) [28], etc. However, the structure of neural networks is difficult to choose, and the convergence speed greatly affects its correct recognition rate. CHSMM requires that the degradation data should conform to a Gaussian distribution, which leads to a reduction in the recognition accuracy. SVM and SOMM need extensive optimization algorithms to estimate model parameters. Furthermore, their implementation depends on sample data in different states, while how to extract these data is not given.

SVDD, a single-valued classification method developed from SVM, rejects non-target class data by creating a hypersphere of the target class data [29]. It has a fast computational speed, strong robustness, and no Gaussian restriction on the training data [30]. Due to its excellent classification ability, SVDD has been widely applied in fields such as abnormal condition detection [31], fault diagnosis [32], and state interval recognition [33]. Nevertheless, state interval recognition is a multi-classification problem. For this reason, scholars proposed the multi-SVDD algorithm, which builds multiple SVDD classifiers based on clustering results of training samples, and determines its class by the distance discriminant function from the test sample to one single-class classifier [34]. The multi-SVDD algorithm usually takes the relative distance from the test sample to the single-class classifier as its distance discriminant function. However, there is a case when the minimum relative distance is rather close to the second smallest one. If the minimum relative distance is taken as the only discriminate criterion, a great recognition error will be caused. Because the sample distribution may be

uneven, and the number of samples may be unbalanced. Consequently, a new state interval determination scheme is devised, which exploits the K-means algorithm to divide state intervals and then recognize state intervals by the multi SVDD algorithm with a novel discrimination criterion.

By the above motivation, an improved SbRLP method based on the dynamic variable combination is proposed. The proposed technique incorporates four steps: (1) dividing the state intervals of reference samples through the K-means algorithm; (2) calculating the local sensitivity of each variable in each state interval, and then determining the dynamic variable combination with the interval sensitivity threshold; (3) recognizing the state interval of the test sample through the SVDD method with a novel discrimination criterion; (4) united with the dynamic variable combination and state interval recognition results, predicting the RUL of the test sample through the SbRLP method.

This paper is organized as follows. Section 2 recapitulates the methodology for the proposed SbRLP method. Section 3 introduces the error data of the CNC machine tool feed system and four commonly-used performance evaluation metrics. The prognostic performance of various RUL prediction methods on the error data is thus evaluated and compared. The main conclusions of this study are given in section 4.

2. Methodology

The methodology flowchart for the proposed SbRLP method is described in figure 1. It consists of four steps: state interval division, dynamic variable combination determination, state interval recognition and RUL prediction.

2.1 *State interval division*

Through the statistical analysis of monitoring variables, such as the vibration amplitude of the rolling bearing, the root mean square of the gear vibration amplitude, and the dynamic voltage during BGA packaging degradation, the equipment state can be divided into three-state intervals:

1. stationary period, in which the values of monitoring variables remain at a relatively stable and low level. Namely, they fluctuate slightly near the mean value;
2. degradation period, in which the values of monitoring variables deviate from the mean value with a noticeable upward or downward trend, but the changing trend is relatively slow;
3. failure period, in which the values of monitoring variables seriously deviate from the mean values with an accelerated upward or downward trend, finally leading to the failure.

The k-means algorithm is the best-known divisional clustering algorithm, and its simplicity and efficiency make it often used by the multi-SVDD algorithm to divide state intervals. Thus, based on the monitoring data of reference samples, state intervals are divided by the k-means algorithm and $k = 3$. Then, the state interval endpoint of reference sample $i(i = 1, 2, \ldots, n)$ in state interval $e(e = 1, 2, 3)$ is obtained as K_{ri}^{e}. $K_{ri}^{3} \cdot \Delta t$ is the failure sampling time of reference sample i. n is the number of reference samples, and Δt is the sampling interval.

2.2 *Dynamic variable combination determination*

Generally, the more sensitive one monitoring variable, the greater the change range of its value [35]. Assuming that the number of monitoring variables is m and $X_{ri}^{j} = [x_{ri}^{j}(\Delta t), x_{ri}^{j}(2\Delta t), \ldots, x_{ri}^{j}(K_{ri}^{3} \cdot \Delta t)]$ is the sampling point sequence of monitoring variable $j(j = 1, 2, \ldots, m)$ of reference sample i. Then, based on the value change of variable j in time period $[\Delta t, K_{ri}^{3} \cdot \Delta t]$, its local sensitivity in the stationary period can be defined as,

$$Sen_{j1} = \sum_{i=1}^{n} \frac{x_{ri}^{j}(K_{ri}^{1} \cdot \Delta t) \times \left(x_{ri}^{j}(\Delta t)\right)^{-1}}{(K_{ri}^{1} \cdot \Delta t - \Delta t) \times (\Delta t)^{-1}} \tag{1}$$

where K_{ri}^{1} is the state interval endpoint of reference sample i in the stationary period, and $[\Delta t, K_{ri}^{1} \cdot \Delta t]$ is the time period of the stationary period.

Similarly, local sensitivities of variable j in the degradation period and failure period are respectively obtained as,

$$Sen_{j2} = \sum_{i=1}^{n} \frac{x_{ri}^{j}(K_{ri}^{2} \cdot \Delta t) \times \left(x_{ri}^{j}\left((K_{ri}^{1} - 1) \cdot \Delta t\right)\right)^{-1}}{(K_{ri}^{2} \cdot \Delta t - (K_{ri}^{1} - 1)\Delta t) \times ((K_{ri}^{1} - 1) \cdot \Delta t)^{-1}} \tag{2}$$

$$Sen_{j3} = \sum_{i=1}^{n} \frac{x_{ri}^{j}(K_{ri}^{3} \cdot \Delta t) \times \left(x_{ri}^{j}\left((K_{ri}^{2} - 1) \cdot \Delta t\right)\right)^{-1}}{(K_{ri}^{3} \cdot \Delta t - (K_{ri}^{2} - 1)\Delta t) \times ((K_{ri}^{2} - 1) \cdot \Delta t)^{-1}} \tag{3}$$

where K_{ri}^{2} is the state interval endpoint of reference sample i in the degradation period and K_{ri}^{3} is that in the failure period. $[K_{ri}^{1} \cdot \Delta t, K_{ri}^{2} \cdot \Delta t]$ is the time period of the degradation period and $[K_{ri}^{2} \cdot \Delta t, K_{ri}^{3} \cdot \Delta t]$ is that of the failure period.

Then combined with local sensitivities obtained through equations (1)–(3), the local sensitivity threshold in state interval e can be defined as,

$$SenQ_{e} = G * \max\{Sen_{je} | j = 1, \ldots, m; e = 1, 2, 3\} \tag{4}$$

where G is the percentage of maximum local sensitivity and $0 < G \leq 1$. The larger the value of G, the higher the local

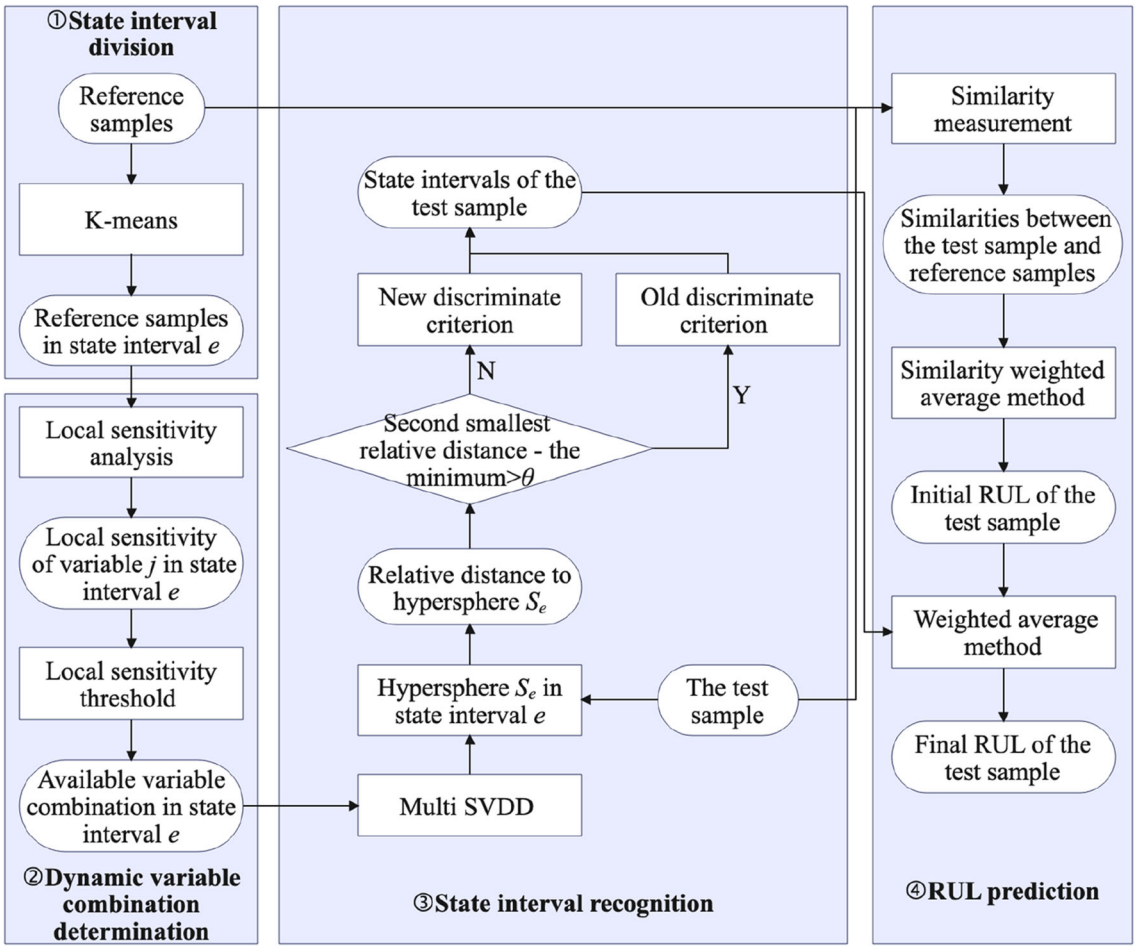

Figure 1. Flowchart of the methodology for the proposed SbRLP method.

sensitivities of extracted monitoring variables. Sen_{je} is the local sensitivity of variable j in state interval e.

If $Sen_{je} \geq SenQ_e$, variable j is available for state interval e, and it is placed in the variable combination of state interval e. Thus, the variable combination of state interval e can be obtained as DB_e.

2.3 *State interval recognition*

Based on reference samples in state interval $e(e = 1, 2, 3)$, hypersphere S_e is established by the multi SVDD algorithm. Assuming that the sampling point of the test sample at time $t = p \cdot \Delta t$ is $x_o(p \cdot \Delta t)$, its distance to hypersphere S_e is d_{ep}, and the radius of hypersphere S_e is R_e, its relative distance to hypersphere S_e can be defined as $H_{ep} = d_{ep}/R_e$. Moreover, assuming that its minimum relative distance is $H_{ep}^{\min 1}$ and its second smallest relative distance is $H_{ep}^{\min 2}$, the new discriminate criterion of the multi SVDD algorithm is:

(1) if $H_{ep}^{\min 2} - H_{ep}^{\min 1} > \theta$, the minimum relative distance is taken as the only discrimination criterion;

(2) if $H_{ep}^{\min 2} - H_{ep}^{\min 1} \leq \theta$, firstly assuming that the hypersphere to which $H_{ep}^{\min 1}$ belongs is $S_\alpha(S_\alpha \in \{S_1, S_2, S_3\})$ and that to which $H_{ep}^{\min 2}$ belongs is $S_\beta\left(S_\beta \in \{S_1, S_2, S_3\}\right)$. θ can be determined through equation (4). Then through the KNN algorithm, L nearest-neighbor sampling points of sampling point $x_o(p \cdot \Delta t)$ are searched from hypersphere S_α and defined as $MINX_{op}^{\alpha} = \left\{\min x_{op}^{1\alpha}, \min x_{op}^{2\alpha}, \ldots, \min x_{op}^{L\alpha}\right\}$. Similarly, its L nearest-neighbor sampling points in hypersphere S_α are obtained as $MINX_{op}^{\beta} = \left\{\min x_{op}^{1\beta}, \min x_{op}^{2\beta}, \ldots, \min x_{op}^{L\beta}\right\}$. Finally, the membership grade $\rho_\alpha(x_o(p \cdot \Delta t))$ of sampling point $x_o(p \cdot \Delta t)$ to hypersphere S_α is calculated through equation (5). So is the membership grade $\rho_\beta(x_o(p \cdot \Delta t))$. If $\rho_\alpha(x_o(p \cdot \Delta t)) \geq \rho_\beta(x_o(p \cdot \Delta t))$,

sampling point $x_o(p \cdot \Delta t)$ belongs to state interval α. Otherwise, it belongs to state interval β.

$$\rho_f(x_o(p \cdot \Delta t)) = \frac{sd_f(x_o(p \cdot \Delta t))}{\left|sd_f(x_o(p \cdot \Delta t)) - 1\right|} \tag{5}$$

where $sd_f(x_o(p \cdot \Delta t))$ is the similarity density of sampling point $x_o(p \cdot \Delta t)$ in hypersphere $S_f(f = \alpha \quad or \quad \beta)$. It represents the ratio of L local proximity density of sampling point $x_o(p \cdot \Delta t)$ in hypersphere S_f to the mean L local proximity density of sampling points in $MINX_{op}^f$, and then it can be defined as,

$$sd_f(x_o(p \cdot \Delta t)) = \frac{L * lden_{Lf}(x_o(p \cdot \Delta t))}{\sum_{l=1}^{L} lden_{Lf}(\min x_{op}^f)} \tag{6}$$

where $lden_{Lf}()$ is L local proximity density of one sampling point in hypersphere S_f. It represents the mean distance of one sampling point to its L nearest-neighbor sampling points in hypersphere S_f, and then the L local proximity density of sampling point $x_o(p \cdot \Delta t)$ in hypersphere S_f can be defined as,

$$lden_{Lf}(x_o(p \cdot \Delta t)) = \frac{\sum_{l=1}^{L} \left\| x_o(p \cdot \Delta t) - \min x_{op}^{lf} \right\|}{L} \tag{7}$$

where $\min x_{op}^{lf}$ denotes the $l(l = 1, 2, \ldots, L)$th nearest-neighbor sampling point of sampling point $x_o(p \cdot \Delta t)$ in hypersphere S_f and $\min x_{op}^{lf} \in MINX_{op}^f$. L is the number of nearest-neighbor sampling points.

2.4 *RUL prediction*

(1) Determining time range D

At time $t = p \cdot \Delta t$, sampling points of the test sample involved in the similarity measurement are,

$$X_o(p, H) = [x_o(p \cdot \Delta t), \ldots, x_o((p - H) \cdot \Delta t)] \tag{8}$$

where $x_o(u \cdot \Delta t) = \left[x_o^1(u \cdot \Delta t), \ldots, x_o^m(u \cdot \Delta t)\right]$ and m is the number of monitoring variables. $u = p, ..., p - H$ and H is a non-negative integer. $D = (H + 1) \cdot \Delta t$ and D can be determined based on the operation experience.

(2) Similarity measurement

Given its practicability and simpleness, the squared Euclidean distance is employed to compute the interval similarity for variable $j(j = 1, 2, \ldots, m)$ between the degradation interval of the test sample in time period $[(p - H) \cdot \Delta t, p \cdot \Delta t]$ and that of reference sample i in time period $[(q - H) \cdot \Delta t, q \cdot \Delta t]$. Thus, the interval similarity $Sim(p, H, i, j, q)$ can be defined as,

$$Sim(p, H, i, j, q) = \sqrt{\sum_{h=0}^{H} \left(x_o^j(p - h) \cdot \Delta t - x_j((q - h) \cdot \Delta t)\right)^2} \tag{9}$$

where $x_{ri}^j((q - h) \cdot \Delta t)$ is the sampling point of reference sample i at time $(q - h) \cdot \Delta t$. $H \le q \le K_{ri}^3$ and $K_{ri}^3 \cdot \Delta t$ is the failure sampling time of reference sample i.

Then for variable j, united with the interval similarity $Sim(p, H, i, j, q)$, the maximum similarity between reference sample i and the test sample at time $t = p \cdot \Delta t$ can be obtained as,

$$Sim_{o \leftrightarrow ri}^j(p) = \min_{H \le q \le K_{ri}^3} Sim(p, H, i, j, q) \tag{10}$$

(3) Initial RUL prediction

For variable j, assuming that $N_{ri}^j(p) \cdot \Delta t$ is the sampling time of reference sample i corresponding to the maximum similarity $Sim_{o \leftrightarrow ri}^j(p)$, and thus,

$$Sim_{o \leftrightarrow ri}^j(p) = \arg\min_q Sim(p, H, i, j, q) \tag{11}$$

Then at time $N_{ri}^j(p) \cdot \Delta t$, the actual RUL of reference sample i is the difference between its failure sampling time and time $N_{ri}^j(p) \cdot \Delta t$. And thus, the actual RUL of reference sample i at time $N_{ri}^j(p) \cdot \Delta t$ can be defined as

$$ARL_{ri}^j(p) = \left(K_{ri}^3 - N_{ri}^j(p)\right) \cdot \Delta t \tag{12}$$

where $K_{ri}^3 \cdot \Delta t$ is the failure sampling time of reference sample i.

Finally, associated with the maximum similarity of reference sample i, the initial RUL of the test sample at time $t = p \cdot \Delta t$ can be obtained through the similarity weighted average method as,

$$PRL_o^j(p) = \frac{\sum_{i=1}^{n} Sim_{o \leftrightarrow ri}^j(p) \cdot \left[\left(K_{ri}^3 - N_{ri}^j(p)\right) \cdot \Delta t\right]}{\sum_{i=1}^{n} Sim_{o \leftrightarrow ri}^j(p)} \tag{13}$$

where $Sim_{o \leftrightarrow ri}^j(p)$ is the maximum similarity between reference sample i and the test sample at time $t = p \cdot \Delta t$.

(4) Final RUL prediction

Assuming that variable combination $DB_e(e = 1, 2, 3)$ includes m_e monitoring variables. If sampling points in $x_o(p, H)$ all belong to state interval e, then united with the local sensitivity of variable $b_e(b_e = 1, 2, ..., m_e)$ in state interval e, the RUL of the test sample at time $t = p \cdot \Delta t$ can be obtained through the weighted average method as,

$$PRL_o^e(p) = \sum_{b_e=1}^{m_e} \frac{Sen_{b_e e}}{\sum_{b_e}^{m_e} Sen_{b_e e}} \cdot PRL_o^{b_e}(p) \tag{14}$$

where $Sen_{b_e e}$ is the local sensitivity of variable b_e in state interval e.

Finally, assuming that there are A_e sampling points in $X_o(p,H)$ belonging to state interval e, then through the weighted average method, the final RUL of the test sample at time $t = p \cdot \Delta t$ can be obtained as,

$$PRL_o(p) = \sum_{e=1}^{3} \frac{A_e}{H} \cdot PRL_o^e(p) \tag{15}$$

where $\sum_{e=1}^{3} A_e = H$.

3. Case analysis

3.1 *Case description*

The case data in this paper is from the failure test of the CNC machine tool feed system conducted by Huazhong University of Science and Technology and Chongqing University. Figure 2 shows the experimental platform of the CNC machine tool feed system, and table 1 gives its basic design parameters. This experimental platform adopts the semi-closed-loop servo motion control, and it tests the actual position of the workbench by the grating ruler, enabling dynamic real-time acquisition of the difference between the rotary encoder and scale position as each axis moves to a set position. The error measurement is carried out every 60 days with the X-axis and Y-axis displacement as its measurement object. Table 2 shows partial error measurement data, which has six groups of error measurement data with a data volume of 318 and a failure life range of [430,550]. Moreover, its failure error threshold is the Y-axis reverse clearance error threshold, i.e., 7.84. In table 2, Y_1 is the X-axis positioning error, Y_2 is the Y-axis positioning error, Y_3 is the X-axis straightness error, Y_4 is the Y-axis straightness error, Y_5 is the X-axis reverse clearance error, and Y_6 is the Y-axis reverse clearance error. Take the first five groups of error measurement data in table 2 as reference samples and the last group as the test sample.

Four commonly-used metrics are employed to evaluate the prediction performance of the proposed method, namely the absolute error (*AE*), the mean absolute error (*MAE*), the root mean square error (*RMSE*), and the score function (*Score*). *AE* measures the prediction performance of the proposed method at a single sampling point, while the rest is the global performance. $AE()$ is the absolute value of the error between the actual and predicted value at some sampling point, and it is shown as,

$$AE(p) = |PRL(p) - ARL(p)| \tag{16}$$

where $ARL(p)$ is the actual RUL of sampling point p and $PRL(p)$ is its predicted RUL. $p = 1, 2, ..., N$ and N is the number of sampling points. The smaller the $AE()$, the better the prediction performance of the proposed method at some sampling point.

MAE is the mean absolute value of errors between actual and predicted values, and *RMSE* is the mean value of their squared error. The smaller the *MAE* and *RMSE*, the lower the prediction error of the proposed method and the higher its prediction accuracy. Then their expressions are given by,

$$MAE = \frac{1}{N}\sum_{p=1}^{N} |PRL(p) - ARL(p)| \tag{17}$$

$$RMSE = \frac{1}{N}\sum_{p=1}^{N} (PRL(p) - ARL(p))^2 \tag{18}$$

Score shows different penalties for different prediction errors. Under the same error, the penalty of the overestimated RUL is greater than that of the underestimated RUL because the catastrophic consequence of untimely maintenance is much more severe than that of excessive maintenance. This difference is in line with the risk-averse nature of equipment maintenance. Thus, the smaller the *Score*, the more accurate the prediction results of the proposed method. Then its expression is given by,

$$Score = \begin{cases} \sum_{p=1}^{N} \left(e^{-(PRL(p)-ARL(p))/13} - 1\right) & PRL(p) < ARL(p) \\ \sum_{p=1}^{N} \left(e^{(PRL(p)-ARL(p))/10} - 1\right) & PRL(p) \geq ARL(p) \end{cases} \tag{19}$$

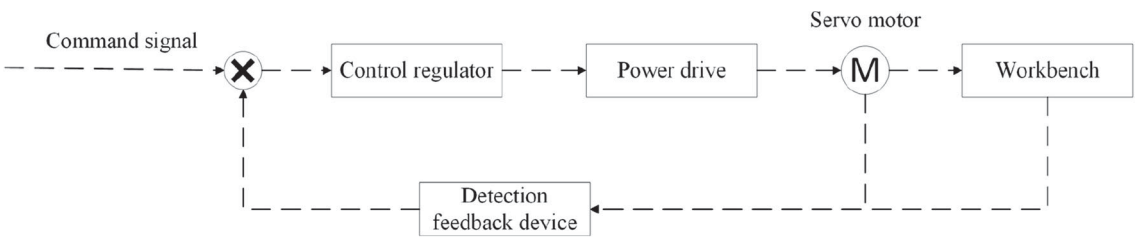

Figure 2. The experimental platform of the CNC machine tool feed system.

Table 1. The design parameters of the experimental platform in figure 1.

Parameter	Value	Parameter	Value
Working process in the X-direction	300 mm	Minimum data acquisition cycle	0.5 ms
Working process in the Y-direction	500 mm	Length*width*height	1000 mm*750 mm*1000 mm
Repetitive positioning accuracy	5 um	Interpolation timer pulses	2 ms

Table 2. The error measurement data of the experimental platform in figure 1.

Group	Time/day	Y_1	Y_2	Y_3	Y_4	Y_5	Y_6
1	0	7.12	14.18	1.8	3.8	2.59	3.92
	60	7.44	14.97	2	4.1	2.8	4.3
	120	7.8	15.2	2.1	4.5	3.4	4.5
	180	7.5	13.8	2.4	5.3	3.5	4.8
	240	9.6	18.2	2.6	6	4.2	5.6
	300	8.7	16.7	2.9	6.4	4.4	6.3
	360	11.4	21.7	3.3	7.1	5.4	7.4
	420	10.4	20	3.5	7.5	5.9	8
				……			
6	540	13.32	28.24	4.24	7.92	7.11	8.05

3.2 *RUL prediction*

(1) Dynamic variable combination determination

The state intervals of reference samples are divided by the K-means algorithm and shown in table 3. Based on reference samples in table 3 and their state intervals, the local sensitivity of each variable in each state interval is calculated through equations (1)–(3) and shown in table 4. Figure 3 also provides the comparison result about interval sensitivities of different variables. Then, in the light of interval sensitivities in table 4, the interval sensitivity threshold in each state interval is calculated through equation (4) and shown in table 4, in which $G = 0.9$. Finally, according to interval sensitivity thresholds in table 4, the available variable combination in each state interval is obtained and shown in table 4.

(2) State interval identification

Firstly, based on reference samples in table 3 and dynamic variable combinations in table 4, the SVDD model in each state interval is trained, and the training results are concluded in table 5. Table 5 also gives parameters of multi SVDD training models with all variables. Then, the test sample is inputted into multi SVDD training models to obtain its relative distances, as shown in table 6. Meanwhile, according to the maximum difference between the second smallest relative distance and the minimum one in table 6, the relative distance difference threshold θ is calculated through equation (4) and $\theta = 1.59$, where $G = 0.9$. Finally, by comparing the relative distance difference of each sampling point with the threshold θ, preliminary state interval recognition results can be obtained and shown in table 6. In table 6, the relative distance differences of sampling points 4, 5, and 7 are less than the threshold θ, which means their state intervals require further determination by the new discrimination criterion. In addition, table 7 gives the state interval recognition results with all variables for comparison.

To further recognize the "uncertainty" in table 6, their l nearest-neighbor sampling points are screened from their

Table 3. The state intervals of reference samples.

Group	Time/day	Y_1	Y_2	Y_3	Y_4	Y_5	Y_6	State interval
1	0	7.12	14.18	1.8	3.8	2.59	3.92	Stationary period
	60	7.44	14.97	2	4.1	2.8	4.3	Stationary period
	120	7.8	15.2	2.1	4.5	3.4	4.5	Stationary period
	180	7.5	13.8	2.4	5.3	3.5	4.8	Stationary period
	240	9.6	18.2	2.6	6	4.2	5.6	Degradation period
	300	8.7	16.7	2.9	6.4	4.4	6.3	Degradation period
	360	11.4	21.7	3.3	7.1	5.4	7.4	Failure period
	420	10.4	20	3.5	7.5	5.9	8	Failure period
				……				
5	480	13.7	26.68	4.02	7.79	6.77	8.01	Failure period

Table 4. The dynamic variable combination.

State interval	Local sensitivity						Local sensitivity threshold	Dynamic variable combination
	Y_1	Y_2	Y_3	Y_4	Y_5	Y_6		
Stationary period	0.066	0.067	0.079	0.078	0.078	0.076	0.071	Y_3, Y_4, Y_5, Y_6
Degradation period	0.780	0.824	0.875	0.869	0.904	0.885	0.814	Y_2, Y_3, Y_4, Y_5, Y_6
Failure period	0.860	0.857	0.870	0.883	0.899	0.893	0.809	$Y_1, Y_2, Y_3, Y_4, Y_5, Y_6$

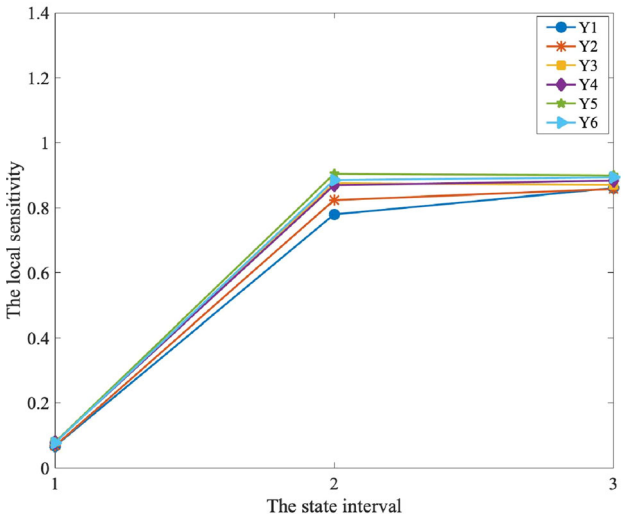

Figure 3. The local sensitivities of different variables.

identified state interval data by the KNN algorithm. $l = 6$, and it is determined according to Yuan *et al* [36]. Then, the membership degree of each identified sampling point to its identified state interval is calculated through equations (5)–(7). Table 8 gives l local proximity densities, density similarities, and membership degrees of identified sampling points. Finally, based on the maximum membership principle, state intervals of identified sampling points are determined and shown in table 8. In addition, table 9 provides the state interval identification results of the test sample by different discriminant criteria.

(3) RUL prediction

Based on the local sensitivities in table 4 and the state interval recognition results by the new discriminant criteria in table 9, the RULs of the test sample are predicted through equations (8)–(15) and shown in figure 4. Figure 4 also gives its actual RULs as the benchmark. To verify the effectiveness and superiority of the proposed SbRLP method, figure 5 provides AEs of the proposed SbRLP method, the classical SbRLP method, and the proposed SbRLP method with the old discrimination criterion. Moreover, table 10 summarizes their MAEs, RMSEs, and Scores in different state intervals and the whole life cycle. Additionally, to further validate the prediction performance of the proposed SbRLP method, it is compared with non-SbRLP methods commonly-used in RUL prediction, including the backpropagation (BP) neural networks, SVR, and GM (1, N). Moreover, figure 6 shows their AEs, and table 11 lists a summary of their MAEs, RMSEs, and Scores.

3.3 *Result analysis*

As can be seen from table 4, the same variable has different sensitivities in different state intervals. For example, variable Y_3 has a sensitivity of 0.066 in the stationary period, 0.780 in the degradation period, and 0.860 in the failure period. And different variables have different sensitivities in the same state interval. For example, the sensitivity ranking in the stationary period is $Y_3 > Y_4 > Y_5 > Y_6 > Y_2 > Y_1$, but that in the degradation period and the failure period are respectively $Y_5 > Y_6 > Y_3 > Y_4 > Y_2 > Y_1$ and $Y_5 > Y_6 > Y_4 > Y_3 > Y_1 > Y_2$. In figure 3, the sensitivity trends of different variables are also different. For example,

Table 5. Parameters of the SVDD training models.

Type	State interval	Radius R	Sphere center
The dynamic variable combination	Stationary period	0.2285	(0.4933, 0.5210, 0.4203, 0.4750)
	Degradation period	0.2426	(0.8165, 0.8860, 0.8775, 0.8305, 0.8561)
	Failure period	0.3085	(0.8873, 0.8113, 0.8912, 0.8774, 0.8468, 0.8804)
All variables	Stationary period	0.2664	(0.5569, 0.5088, 0.5084, 0.5093, 0.4276, 0.4089)
	Degradation period	0.2510	(0.6921, 0.6588, 0.6899, 0.6906, 0.6088, 0.7018)
	Failure period	0.3085	(0.8873, 0.8113, 0.8912, 0.8774, 0.8468, 0.8804)

Table 6. The state interval recognition results of the test sample under the dynamic variable combination.

Sampling point	H_1	H_2	H_3	Difference between the second smallest relative distance and the minimum one	State interval
1	1.333	6.891	4.982	3.648	Stationary period
2	0.375	6.494	3.817	3.442	Stationary period
3	0.305	5.883	2.534	2.229	Stationary period
4	0.817	4.979	1.351	0.533	Uncertainty
5	1.754	3.868	0.580	1.174	Uncertainty
6	3.402	2.215	0.367	1.848	Degradation period
7	5.256	0.805	1.514	0.709	Uncertainty
8	5.676	0.820	2.581	1.761	Failure period
9	6.767	0.790	4.087	3.298	Failure period
10	7.315	1.767	5.306	3.539	Failure period

Table 7. The state interval recognition results of the test sample under all variables.

Sampling point	H_1	H_2	H_3	Difference between the second smallest relative distance and the minimum one	State interval
1	1.354	11.235	5.387	4.034	Uncertainty
2	0.439	8.608	5.190	4.751	Uncertainty
3	0.409	5.715	4.834	4.425	Uncertainty
4	0.978	3.047	4.283	2.069	Uncertainty
5	1.905	1.308	3.605	0.597	Uncertainty
6	3.596	0.828	2.248	1.420	Uncertainty
7	5.032	3.415	1.185	2.230	Uncertainty
8	5.618	5.821	0.833	4.785	Uncertainty
9	6.176	9.218	0.708	5.467	Failure period
10	6.429	11.965	1.353	5.076	Failure period

the sensitivities of variables Y_1, Y_2, Y_4, and Y_6 increase monotonically with the equipment performance degradation, while these of variables Y_3 and Y_6 increase and then decrease. These differences mean that the type and number of available degradation variables will vary with the state interval, proving the necessity of considering the dynamic variable combination and the rationality of constructing the dynamic variable combination based on the sensitivity differences of variables in different state intervals. Additionally, in table 4, the variable combination in each state interval does differ. This difference further demonstrates that it is needful and effective to construct the dynamic variable combination based on the local sensitivities of variables.

According to the comparison result in table 5, the radiuses under the dynamic variable combination are less than those under all variables, which means that the former has better data convergence. Tables 6 and 7 show that the amount of "uncertainty" under the dynamic variable combination is much less than that under all variables. These indicate that compared with using all variables, considering the dynamic variable combination can help eliminate useless monitoring information and finally more accurately recognize state intervals of the test sample, proving the superiority of constructing the dynamic variable combination. Furthermore, in figure 5, both the proposed SbRLP method and that with the old discriminate criterion have smaller AEs when opposed to the classical SbRLP method. In table 10, whether in the whole life cycle

Table 8. The state interval recognition results of identified sampling points.

Sampling point	Local proximity density			Density similarity			Membership degree			State interval
	$lden_1$	$lden_2$	$lden_3$	sd_1	sd_2	sd_3	ρ_1	ρ_2	ρ_3	
4	0.068	0.211	/	0.685	1.488	/	2.173	3.050	/	Degradation period
5	0.140	0.139	/	1.395	0.985	/	3.531	66.103	/	Degradation period
7	/	0.246	0.100	/	1.630	0.774	/	2.588	3.423	Failure period

Table 9. The state interval recognition results of the test sample by different discriminant criteria.

Sampling point	The new discriminant criteria	The old discriminant criteria
1	Stationary period	Stationary period
2	Stationary period	Stationary period
3	Stationary period	Stationary period
4	Degradation period	Stationary period
5	Degradation period	Degradation period
6	Degradation period	Degradation period
7	Failure period	Failure period
8	Failure period	Failure period
9	Failure period	Failure period
10	Failure period	Failure period

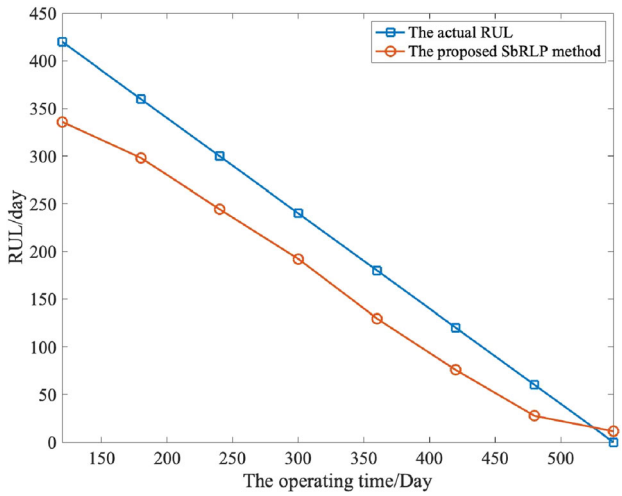

Figure 4. The predicted RULs of the test sample.

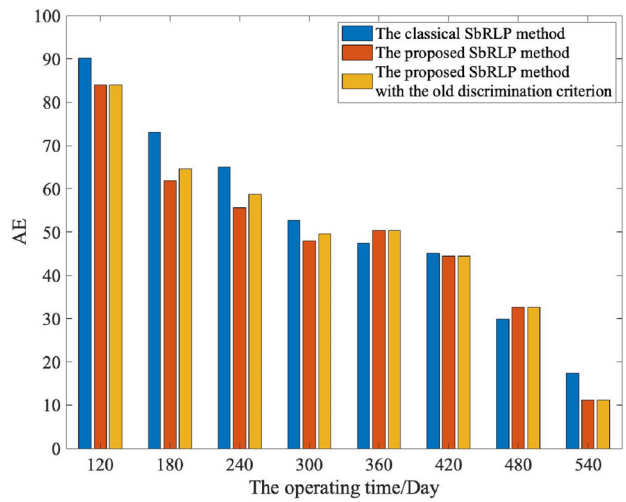

Figure 5. AEs of different SbRLP methods.

or individual state interval, their MAEs, RSMEs, and Scores are also smaller. These indicate that considering the dynamic variable combination can help to obtain more accurate RUL prediction results, further demonstrating the superiority of considering the dynamic variable combination.

Known from figure 5, AEs of the proposed SbRLP method are less than or equal to those of the proposed SbRLP method with the old discriminant criterion. In table 10, its MAE, RSME, and Score of the proposed SbRLP method are also smaller whether in the whole life cycle or individual state interval. These indicate that more accurate RUL prediction results can be obtained with the implementation of the new discriminant criterion, which provides evidence for the effectiveness and superiority of the new discriminant criterion.

The above analysis of figure 5 and table 10 shows that, compared with other SbRLP methods, the proposed SbRLP method has smaller AEs, MAE, RSME, and Score. This indicates that the proposed SbRLP method has higher prediction accuracy and better prediction performance. Furthermore, in table 10, the MAE, RSME, and Score of the proposed SbRLP method are smaller than the classical method in the stationary and degradation period. The opposite is true in the failure period, but their difference is insignificant. This indicates that the proposed SbRLP method can significantly improve the prediction performance of similarity-based RUL prediction in the early to mid-stage equipment performance degradation.

As shown in figure 6 and table 11, the prediction accuracy of the proposed SbRLP method is not the highest compared to the commonly-used non-SbRLP methods. Nevertheless, its prediction results are still good, and it performs well in terms of RMSE. For example, the proposed SbRLP method has smaller PEs, MAE, RSME, and Score than SVR. When opposed to the BP neural network, although the proposed SbRLP method has larger MAE and Score, its most PEs and RSME are minor, and their MAE difference is insignificant. Compared with GM (1, N), its most AEs, MAE, and RSME are smaller, except for the Score. These further prove that the proposed SbRLP method has the capability of obtaining more accurate RUL prediction results. In addition, SVR is for small samples, and thus its prediction error should be smaller than that of BP neural networks because the sample size in this paper is not large. However, its prediction results in figure 6 and table 11 are not satisfactory due to the inappropriate kernel function. This illustrates the importance of selecting a suitable kernel function, which is not a problem for the proposed SbRLP method, and thus further demonstrates its superiority.

Table 10. MAPEs, RMSEs, and Scores of different SbRLP methods.

State interval	Methods	MAPE	RMSE	Score
Stationary period	The classical SbRLP method	81.626	6734.574	649.499
	The proposed SbRLP method	72.919	5439.452	376.732
	The proposed SbRLP method with the old discriminate criterion	74.287	5612.477	390.389
Degradation period	The classical SbRLP method	58.888	3505.582	102.316
	The proposed SbRLP method	51.716	2689.584	54.808
	The proposed SbRLP method with the old discriminate criterion	54.167	2955.332	67.608
Failure period	The classical SbRLP method	34.937	1369.500	20.543
	The proposed SbRLP method	34.653	1424.924	22.497
	The proposed SbRLP method with the old discriminate criterion	34.653	1424.924	22.497
The whole life cycle	The classical SbRLP method	50.804	55.154	1585.802
	The proposed SbRLP method	48.485	52.390	953.068
	The proposed SbRLP method with the old discriminate criterion	49.440	53.437	1005.981

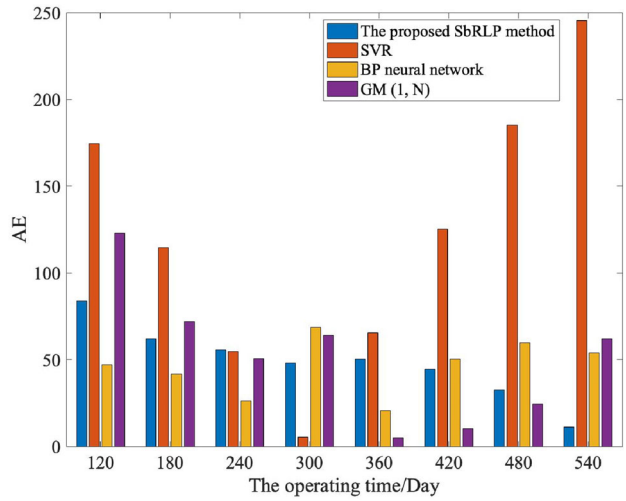

Figure 6. AEs of the proposed SbRLP method and non-SbRLP methods.

Table 11. MAPEs, RMSEs, and Scores of the proposed SbRLP method and non-SbRLP methods.

Methods	MAPE	RMSE	Score
The proposed SbRLP method	48.485	52.390	953.068
SVR	121.355	227.172	686358.52
BP neural network	45.977	202.089	472.860
GM (1, N)	51.429	62.799	111.235

4. Conclusion and future works

This paper raises a novel SbRLP method based on the dynamic variable combination and applies it to the RUL prediction of the CNC machine tool feed system. Its comparison results with different RUL prediction methods show that:

1. through comparison with the classical SbRLP method, considering the dynamic variable combination is necessary. Moreover, it can more accurately recognize the state intervals of the test sample and obtain more accurate RUL prediction results.
2. When opposed to the old discriminate criterion, the new discriminate criterion of the multi SVDD algorithm can help improve the prediction accuracy of the proposed SbRLP method.
3. Compared with other SbRLP methods, the proposed SbRLP method has higher prediction accuracy and can significantly improve the prediction performance of similarity-based RUL prediction in the early and middle stages of equipment performance degradation.
4. Contrasted with non-SbRLP methods, the prediction performance of the proposed SbRLP method is not the best. Nevertheless, its prediction effect is acceptable, and it has an excellent performance in terms of RMSE.

The determination of the dynamic variable combination is a complex problem. This paper takes sensitivity as the only evaluation index. In the future, we will strive to introduce more indexes such as robustness and monotonicity to construct the dynamic variable combination.

Funding: The paper is financially supported by the Zhejiang Natural Science Foundation (Project Number: Q20G010021).

Declarations

Conflict of interest The authors declare that they have no conflict of interest.

References

[1] Ma B, Yan S, Wang X, Chen J and Zheng C 2020 Similarity-based failure threshold determination for system residual life prediction. *Eksploat. Niezawodn.* 22(3): 520–529

[2] Wang H, Chen J H, Qu J and Ni G 2020 A new approach for safety life prediction of industrial rolling bearing based on state recognition and similarity analysis. *Safety Sci.* 122: 104530

[3] Ge J, Sun Y and Zhou S 2015 Fatigue life estimation under multiaxial random loading by means of the equivalent Lemaitre stress and multiaxial S-N curve methods. *Int. J. Fatigue* 79: 65–74

[4] He L, Yu L, Zhu S P, Ding L and Huang H Z 2016 Probabilistic fatigue life prediction of turbine disc considering model parameter uncertainty. *Int. J. Turbo Jet Eng.* 33(2): 87–94

[5] Yu W, Kim I Y and Mechefske C 2020 An improved similarity-based prognostic algorithm for RUL estimation using an RNN autoencoder scheme. *Reliability Engineering Syst. Safe* 199: 106926

[6] Swanson D C, Spencer J M and Arzoumanian S H 2000 Prognostic modelling of crack growth in a tensioned steel band. *Mech. Syst. Signal Pr.* 14(5): 789–803

[7] Orchard M E and Vachtsevanos G J 2007 A particle filtering approach for on-line failure prognosis in a planetary carrier plate. *Int. J. Fuzzy Log. Intell.* 7(4): 221–227

[8] Chen G, Chen J, Zi Y, Pan J and Han W 2018 An unsupervised feature extraction method for nonlinear deterioration process of complex equipment under multi-dimensional no-label signals. *Sensor Actuat. A-Phys.* 269: 464–473

[9] Li X, Ding Q and Sun J Q 2018 Remaining useful life estimation in prognostics using deep convolution neural networks. *Reliab. Eng. Syst. Safe* 172: 1–11

[10] Chen Z, Cao S and Mao Z 2018 Remaining useful life estimation of aircraft engines using a modified similarity and supporting vector machine (SVM) approach. *Energies* 11(1): 28

[11] Liu J, Djurdjanovic D, Ni J, Casoetto N and Lee J 2007 Similarity based method for manufacturing process performance prediction and diagnosis. *Comput. Ind.* 58(6): 558–566

[12] Yu W, Kim I Y and Mechefske C 2020 An improved similarity-based prognostic algorithm for RUL estimation using an RNN autoencoder scheme. *Reliab. Eng. Syst. Safe* 199: 106926

[13] You M Y and Meng G 2013 Toward effective utilization of similarity based residual life prediction methods: weight allocation, prediction robustness, and prediction uncertainty. *Proc. Inst. Mech. Eng. E J. Pro.* 227(1): 74–84

[14] Malinowski S, Chebel-Morello B and Zerhouni N 2015 Remaining useful life estimation based on discriminating shapelet extraction. *Reliab. Eng. Syst. Safe* 142: 279–288

[15] Liu Y, Hu X and Zhang W 2019 Remaining useful life prediction based on health index similarity. *Reliab. Eng. Syst. Safe* 185: 502–510

[16] Hou M, Pi D and Li B 2020 Similarity-based deep learning approach for remaining useful life prediction. *Measurement* 159: 107788

[17] Zhao H L and Chen T M 2022 Engine life prediction based on two-scale similarity. *J. Propuls. Tech.* http://kns.cnki.net/kcms/detail/11.1813.V.20220127.0819.002.html

[18] Liang Z M, Gao J M and Jiang H Q 2019 A maintenance support framework based on dynamic reliability and remaining useful life. *Measurement* 147: 106835

[19] Wang K, Guo Y Q, Zhao W L, Zhou Q F and Guo P F 2022 Remaining useful life prediction of aeroengine based on SSAE and similarity matching. *J. B. Univ. Aeronaut.* https://doi.org/10.13700/j.bh.1001-5965.2021.0741

[20] Yu Q Y, Li J, Dai H D and Xin F L 2022 Lasso based variable selection for similarity remaining useful life prediction of aero-engine. *J. Aerosp. Power.* https://doi.org/10.13224/j.cnki.jasp.20210516

[21] Zhang B, Zhang L and Xu J 2016 Degradation feature selection for remaining useful life prediction of rolling element bearings. *Qual. Reliab. Eng. Int.* 32: 547–554

[22] Gu M Y and Chen Y L 2018 A multi-indicator modeling method for similarity-based residual useful life estimation with two selection processes. *Int. J. Syst. Assur. Eng. Manage.* 9(5): 987–998

[23] Zhang B 2016 *Research on Data-Driven Performance Degradation Modelling and Remaining Useful Life Prediction for Mechanical Equipment*. PhD Thesis. University of Science and Technology Beijing, China. 1-125

[24] Nakamura T, Nagai T, Mochihashi D, Kobayashi I, Asoh H and Kaneko M 2017 Segmenting continuous motions with hidden semi-markov models and gaussian processes. *Front. Neurorobotics* 11: 67

[25] Kim H E, Tan A C, Mathew J and Choi B K 2012 Bearing fault prognosis based on health state probability estimation. *Expert. Syst. Appl.* 39(5): 5200–5213

[26] Yu J 2011 A hybrid feature selection scheme and self-organizing map model for machine health assessment. *Appl. Soft Comput.* 11(5): 4041–4054

[27] Cerrada M, Sánchez R V, Li C, Pacheco F, Cabrera D, de Oliveira J V and Vásquez R E 2018 A review on data-driven fault severity assessment in rolling bearings. *Mech. Syst. Signal Pr.* 99: 169–196

[28] Pan Y N, Chen J and Guo L 2009 Robust bearing performance degradation assessment method based on improved wavelet packet-support vector data description. *Mech. Syst. Signal Pr.* 23(3): 669–681

[29] Wang X H, Wang Y J, Deng X G, Cao Y P and Wang P 2022 Batch process monitoring based on multi-phase and multi-kernel support vector data description. *J. China Univ. Petrol. (Nat. Sci.)* 44(04): 182–188

[30] Zhu X, Zhang Y and Zhu Y 2013 Bearing performance degradation assessment based on the rough support vector data description. *Mech. Syst. Signal Pr.* 34(1–2): 203–217

[31] Zhang Z and Deng X 2021 Anomaly detection using improved deep SVDD model with data structure preservation. *Pattern Recogn. Lett.* 148: 1–6

[32] Zhang C, Peng K and Dong J 2019 A novel plant-wide process monitoring framework based on distributed Gap-SVDD with adaptive radius. *Neurocomputing* 350: 1–12

[33] Chen P and Zhao X Q 2021 Performance degradation evaluation method of rolling bearing based on GLNPE-SVDD. *J. Huazhong Univ. Sci. T.* 49(01): 12–16

[34] Chen S G, Guan Y G, Zhang X Q, Yang Y W and Zhang Y M 2018 Diagnosis method of high voltage isolating switch fault based on multi-SVDD under incomplete fault type. *T. China Elec. Soc.* 33(11): 2439–2447

[35] Zhao H L, Chen T M and Zheng N 2021 Residual useful life estimation based on multi-stage similarity of comprehensive index. *J. Syst. Eng. Electron.* 43(05): 1430–1436

[36] Yuan Y, Cao H, Zhang Y, Xie Q and Yao R 2016 Outlier mining based on neighbor-density-deviation with minimum hyper-sphere. *Inf. Technol. Control.* 45(3): 267–277